Cement and Concrete Composites 81 (2017) 66–76

Contents lists available at ScienceDirect

Cement and Concrete Composites

journal homepage: www.elsevier.com/locate/cemconcomp

The durability of cementitious composites containing microencapsulated phase change materials

Zhenhua Wei [a], Gabriel Falzone [a], Bu Wang [a], Alexander Thiele [b], Guillermo Puerta-Falla [a], Laurent Pilon [b], Narayanan Neithalath [c], Gaurav Sant [a, d, e, *]

[a] Laboratory for the Chemistry of Construction Materials (LC^2), Department of Civil and Environmental Engineering, University of California, Los Angeles, CA 90095, United States
[b] Department of Mechanical and Aerospace Engineering, University of California, Los Angeles, CA 90095, United States
[c] School of Sustainable Engineering and the Built Environment, Arizona State University, Tempe, AZ 85287, United States
[d] California NanoSystems Institute, University of California, Los Angeles, CA 90095, United States
[e] Department of Materials Science and Engineering, University of California, Los Angeles, CA 90095, United States

ARTICLE INFO

Article history:
Received 12 August 2016
Received in revised form
25 March 2017
Accepted 27 April 2017
Available online 1 May 2017

Keywords:
Phase change materials
Cement paste
Concrete
Durability
Enthalpy

ABSTRACT

This study investigates the durability of cementitious composites containing microencapsulated phase change materials (PCMs). First, the stability of the PCM's enthalpy of phase change was examined. A reduction of around 25% in the phase change enthalpy was observed, irrespective of PCM dosage and aging. Significantly, this reduction in enthalpy was not caused by mechanical damage that was induced during mixing, but rather by chemical interactions with dissolved SO_4^{2-} ions. Second, the influence of PCM additions on water absorption and drying shrinkage of PCM-mortar composites were examined. PCM microcapsules reduced the rate and extent of water sorption; the former was due to their non-sorptive nature which induces hindrances in moisture movement, and the latter was due to dilution, i.e., a reduction in the volume of sorptive cement paste. On the other hand, PCM inclusions did not influence the drying shrinkage of cementitious composites, due to their inability to restrain the shrinkage of the cement paste. The results suggest that PCMs exert no detrimental influences on, and, in specific cases, may even slightly improve the durability of cementitious composites.

1. Introduction and background

Heating, ventilation, and air conditioning of buildings accounts for nearly 20% of annual energy consumption in the U.S. [1]. The embedment of phase change materials (PCMs) in building materials is an effective means to reduce such energy expenditures [2–6]. The benefits of energy efficiency arise from the ability of PCMs to store and release heat in response to temperature changes by undergoing reversible phase transitions between the solid and liquid states. Organic compounds such as paraffins and fatty acids are often used as PCMs due to their low cost, high latent heat of fusion, and appropriate temperature of phase change (T_{pc}) [4,6]. These materials are generally used in microencapsulated forms (with particle diameter of 1 μm-1 mm) to facilitate handling and to prevent PCM exposure with caustic building materials [4].

The economic feasibility of employing microencapsulated PCMs in cementitious composites (i.e., PCM-mortar composites) depends on the ability of PCMs to reduce energy expenditures while embedded within a structural material [7]. Therefore, the PCM must retain its enthalpy of phase change over the service life of the composite. This requires the following: (i) physical durability of PCM capsules, i.e., the ability to resist rupture during concrete mixing and during thermal cycling, and (ii) chemical stability of the PCM microcapsules within the alkaline cementitious environment [8–10]. Moreover, the dosage of the PCMs should not detrimentally influence the durability of the cementitious matrix in which they are embedded.

Numerous studies have examined the ability of PCMs to reduce energy needs that are associated with heating/cooling buildings [2–6,11]. A smaller body of research has examined the ability of PCMs to mitigate early-age temperature rise in cementitious materials caused by exothermic cement hydration, and the resultant

* Corresponding author. Laboratory for the Chemistry of Construction Materials (LC^2), Department of Civil and Environmental Engineering, University of California, Los Angeles, CA 90095, United States.
E-mail address: gsant@ucla.edu (G. Sant).

http://dx.doi.org/10.1016/j.cemconcomp.2017.04.010
0958-9465/

risk of thermal cracking [12–14]. In spite of extensive efforts, only a few studies have examined the durability of PCMs in the context of their chemical durability in alkaline cementitious environments [12,15]. During hydration, cement particles dissolve, turning the pore solution into a caustic electrolyte [16]. The pore solution contains alkalis, SO_4^{2-}, and Ca^{2+} species, presenting a pH typically greater than 13 [17–19]. When microencapsulated PCMs are embedded in such caustic systems, chemical reactions between the pore solution and the capsule shell could result in damaging alterations, which could reduce the enthalpy of phase change [12]. Thus, it is of great importance to investigate the extent to which exposure to caustic cementitious environments affects microencapsulated PCMs' thermal storage capability. With these considerations in mind, the present study systematically examines:

- ***PCM survivability during fabrication of PCM-mortar composites,*** with respect to damage and/or rupture of the PCM microcapsules that may occur during mechanical mixing,
- ***Chemical durability of PCM within cementitious matrices,*** and the potential interactions between the PCM and the pore-fluid that results in enthalpy alteration (reduction), and
- ***Cementitious matrix durability,*** with emphasis on assessing how dosage of PCMs alters water absorption and drying shrinkage behavior of cementitious composites containing PCMs.

Based on this direction of inquiry, a 25% reduction in enthalpy of phase change of PCMs is noted following their embedment in a cementitious matrix, regardless of whether mechanical mixing is carried out or not. This observed enthalpy reduction is attributed to chemical reaction of the PCM shell material with sulfate ions, causing the release of core material, and its reaction with the pore solution. To the best of our knowledge, this is the first time that a reduction in enthalpy of phase change of PCMs in cementitious environments and its mechanism have been reported. Additionally, we observe that PCMs only minimally influence the drying shrinkage of PCM-mortar composites, while beneficially reducing water sorption similar to other non-sorptive inclusions. These latter parameters which reflects the tightness of concrete to aggressive agents [20–25] and its resistance to cracking, respectively, are critical indicators of concrete durability [26–29].

2. Materials and methods

2.1. Materials

Four different commercially available microencapsulated PCMs were used: MPCM6D, MPCM24D, MPCM43D (Microtek Laboratories) and Micronal DS 5008X (BASF Corporation). The relevant onset melting temperatures (indicative of T_{pc}) were 4.1 °C, 19.6 °C, 41.2 °C, and 22.8 °C, respectively, as measured by differential scanning calorimetry (DSC). The Microtek PCMs consisted of paraffin (alkane) cores that are encapsulated within melamine-formaldehyde (MF) shells, while the BASF PCM consisted of a paraffin (alkane) core that was encapsulated within an acrylate polymer shell. In each case, variations in the phase change temperature are realized by altering the "chain length", i.e., the number of carbon atoms in an alkane of generic composition (C_nH_{2n+2}, where 'n' is the number of carbon atoms). The PCMs were received in the form of dry powders.

These four microencapsulated PCMs were selected for study since they encompass the range of phase change temperatures relevant for use in cementitious composites. Specifically, T_{pc} near 0 °C (e.g., MPCM6D) may be beneficial to mitigate freeze-thaw damage [30], T_{pc} close to room temperature (e.g., MPCM24D and Micronal DS 5008X) may be beneficial in reducing HVAC-related energy expenditures [6], and a higher T_{pc} (e.g., MPCM43D) may be used to mitigate early-age temperature rise caused by (exothermic) cement hydration [12]. Each of the microencapsulated PCMs has been characterized in detail, e.g., in terms of: (i) their particle size distributions using static light scattering, (ii) their surface morphology using scanning electron microscopy (SEM), and (iii) their enthalpy of phase change using DSC; before and after immersion in alkaline solutions.

To more comprehensively assess chemical stability, MPCM24D was also immersed in sulfate-rich solutions, and examined morphologically using SEM and for compositional changes using X-ray diffraction (XRD). Further, MPCM24D-mortar composites were examined in terms of both their drying shrinkage and water sorption behavior. Broadly, all other PCMs are expected to show similar behavior as MPCM24D based composites due to their similar shell/alkane-core compositions.

An ASTM C150 [31] compliant Type I/II ordinary Portland cement (OPC) was mixed with deionized (DI) water to prepare cement pastes and mortars in accordance with ASTM C192 [32]. The OPC had a nominal mass-based mineralogical composition of: 56.5% Ca_3SiO_5, 18.0% Ca_2SiO_4, 11.4% $Ca_4Al_2Fe_2O_{10}$, 6.3% $Ca_3Al_2O_6$, 4.6% $CaCO_3$, 1.2% $CaSO_4$, 1.1% $CaSO_4 \cdot 2H_2O$, 0.5% $CaSO_4 \cdot 0.5H_2O$, and 0.5% CaO. An ASTM C778 [33] compliant graded quartz sand (denoted as quartz hereafter) was used as a stiff, non-sorptive aggregate within the cement mortars.

Reference ("control") plain pastes with water-to-cement ratio (w/c, mass basis) of 0.35, 0.45, and 0.55 were prepared for water absorption measurements. For all other tests, cementitious mortars were prepared at a fixed w/c = 0.45 at various dosages of microencapsulated PCM and/or quartz inclusions. The inclusions were dosed as a percentage of the total composite volume at three levels (i.e., 10, 30 and 55 vol %). These mixtures are denoted by the volume percentage of the type of inclusion present preceded by "P" and/or "Q" corresponding to the PCM and quartz inclusions, respectively. To maintain workability (i.e., to enhance fluidity at high inclusion volume fractions), a commercially available water-reducing admixture (WRA; MasterGlenium 7500, BASF Corporation) was added. The WRA dosage for each mixture was as follows (% of cement mass): P10–0.5%, P30–2.0%, P20 + Q10–1.0%, P10 + Q20–0.5%, P20 + Q35–1.5%, P10 + Q45–1.0%, and Q55–0.5%. All other formulations contained no WRA.

2.2. Experimental methods

Static Light Scattering: A Beckman Coulter Static Light Scattering (SLS) Particle Analyzer (LS13-320) was used to determine the particle size distributions (PSDs) of the OPC, PCM microcapsules, and graded quartz sand used in the specimen preparation, as presented in Fig. 1. Each material was first dispersed into primary particles via ultrasonication in isopropanol that also served as the carrier fluid. The densities of OPC, quartz, Micronal DS 5008X and Microtek microencapsulated PCMs were taken as: 3150 kg/m^3, 2650 kg/m^3, 300 kg/m^3, and 900 kg/m^3, respectively. The complex refractive indices of the OPC, PCMs, and quartz were taken as 1.70 + i 0.10 [34], 1.53 + i 0.00 [35], and 1.54 + i 0.00 [36], respectively. The maximum uncertainty in the PSDs was about 6% based on 6 replicate measurements.

Differential Scanning Calorimetry: The enthalpy of phase change (ΔH_{PC}), and the phase change temperature (T_{PC}) of the PCMs was determined using differential scanning calorimetry (DSC 8500, Perkin Elmer) in accordance with ASTM E1269 [37]. Prior to measurement, temperature and heat flow calibrations were performed using indium and zinc standards. Samples consisting of ≈10 mg of microencapsulated PCMs or PCM-mortar composites

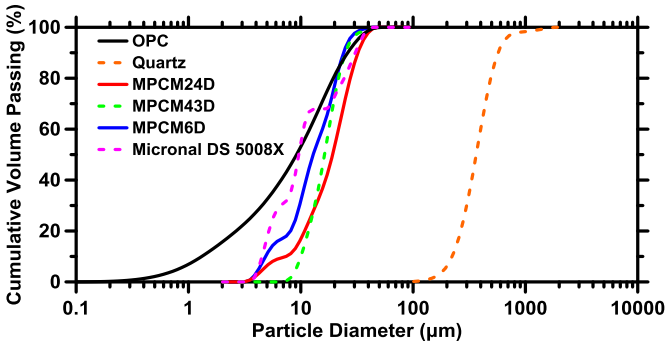

Fig. 1. Particle size distributions of OPC, quartz, and the different microencapsulated PCMs as measured using static light scattering (SLS).

were placed in sealed aluminum pans and subjected to a temperature cycle ranging from −50-to-100 °C at a scan rate of 10 °C/min. The data reported is the average of three replicate specimens.

X-Ray Diffraction: Qualitative X-ray diffraction analysis was performed on PCM microcapsules before and after exposure to alkaline solutions. The samples were scanned from of 5-to-70° (2θ) using a Bruker-D8 Advance diffractometer in a θ-θ configuration with Cu-Kα radiation (λ = 1.54 Å) and a VANTEC-1 detector. The diffractometer was run in continuous mode with an integrated step scan of 0.021° (2θ). A fixed divergence slit of 1.00° was used during X-ray data acquisition.

Scanning Electron Microscopy: SEM observations were performed on pristine PCMs and on PCM capsules before and after immersion in alkaline solutions for 6 h. The microencapsulated PCMs were deposited on carbon adhesive and then gold-coated. Secondary electron (SE) images were obtained at an accelerating voltage of 10 kV and a beam current of 80 pA using an FEI Nova NanoSEM 230.

Water Absorption: A modified ASTM C1585 [38] procedure was used to characterize the rate and extent of water sorption in PCM-mortar composites. Cylindrical specimens (*d* x *h*, 10 cm × 20 cm) were cast, then cured for 28 days in saturated limewater before being cut into 10 cm × 3.75 cm sections using a diamond-tipped masonry saw. The cylindrical slices were conditioned at 50 °C in a desiccator at relative humidity (RH) of 80% established using a saturated KBr solution for 3 days. Thereafter, each sample was stored in a sealed container for another 15 days to allow moisture redistribution. The sides and one face of the cylinder were sealed with aluminum tape, leaving only one open face exposed to water at 23 °C. The mass of water absorbed through this face was recorded over a time period of 8 days using a laboratory balance (ML1502E, Mettler Toledo) with a precision of ±0.01 g. The data reported is the average of three replicate specimens prepared from the same mixing batch.

Drying Shrinkage: Unrestrained drying deformations of cementitious specimens were measured as per ASTM C157 [39]. Cement pastes and mortars were cast in prismatic molds (2.5 cm × 2.5 cm x 28.5 cm, *w* x *h* x *l*), cured for 24 h above water in a sealed container, prior to curing in saturated limewater until an age of 28 days. The specimens were subsequently dried, sealed on two sides with aluminum tape to ensure 1D moisture diffusion, and stored at 25.0 ± 0.2 °C and 50.0 ± 0.2% RH in an environmental chamber (KB024-DA, Darwin Chambers Company). Changes in the prismatic samples' lengths were recorded at 1, 3, 7, 14, 28, 56, and 90 days from the start of the drying period. The data reported is the average of four replicate specimens prepared from the same mixing batch.

3. Results and discussion

3.1. Stability of the PCM's phase change enthalpy in cementitious environments

Fig. 2(a) displays DSC heat flow curves showing the melting and solidification behavior of pristine MPCM24D microcapsules. The curves show small peaks attributed to impurities blended into the paraffin (the active PCM ingredient) to control its phase change temperature [40]. The peak temperature during the melting (heating) process was about 27.8 °C, while the peak temperature during the solidification (cooling) was about 16.6 °C. The difference between observed peak temperatures for melting and solidification is indicative of supercooling, which is common in microencapsulated PCMs, due to the lack of heterogeneous nucleation sites for solidification to initiate within the microcapsules [4–6]. The enthalpies of phase change were 161.2 ± 0.5 kJ/kg and 136.6 ± 0.4 kJ/kg for pristine MPCM24D and Micronal DS 5008X, respectively (for other PCMs, see Supplementary Materials, Section S.1). The data reported is the average of three replicates.

Fig. 2(b) shows DSC heating curves for cement mortar specimens containing 0, 10, 20 and 30 vol % MPCM24D in the mixture. The temperature corresponding to the onset (24 ± 1 °C) of phase change, and the temperature at the peak (27 ± 1 °C) were similar regardless of the PCM dosage. No peaks were observed in the DSC curve of the plain cement paste, as expected. It is worth pointing out that the cooling curves show behavior similar to that of the heating curves, and the enthalpy of solidification is equal and opposite to that corresponding to melting. The microencapsulated PCM mass fraction in the composite dictates its "expected" phase change enthalpy ΔH_{calc} (in kJ/kg) expressed as,

$$\Delta H_{calc} = \frac{m_P h_{sf,P}}{m_P + m_m} \quad (1)$$

where, $h_{sf,P}$ is the measured latent heat of fusion of the core-shell PCM microcapsules (e.g., 161.2 kJ/kg for MPCM24D), while m_P and m_m are the masses of core-shell PCM microcapsules and the cement paste in the composite, respectively. Fig. 2(c) shows the correlation between the measured phase change enthalpy of PCM-containing cementitious composites, ΔH_{exp}, and that calculated using Equation (1), ΔH_{calc}. A linear relation is noted between ΔH_{exp} and ΔH_{calc}, but with a slope of 0.75. As such, the incorporation of PCM microcapsules within the cementitious paste results in a 25% enthalpy reduction, which was observed to be independent of both the PCM dosage and the age of the cementitious composite. A similar enthalpy reduction was observed previously when Micronal DS 5008X PCM microcapsules were added to cement pastes [12].

PCM capsule survivability during mechanical mixing: Mechanical mixing of the PCM-mortar composites, and the potential damage it causes to the PCM microcapsules, was investigated as the cause of the enthalpy reduction observed in Fig. 2(c). As a comparison to PCM mortars that were fabricated by mixing the cement, microencapsulated PCM, and water in a planetary action mixer as per ASTM C305 [41], an additional set of PCM-mortar composites was created within a DSC pan ($\varphi = 5$ mm) by gently sprinkling onto an underlying paste layer, PCM particles, and then covering these particles with additional cement paste, forming a "sandwich", after which the pan was crimped shut. The resulting PCM sandwich specimens were cured for 3 days in a sealed condition prior to DSC characterization. This preparation procedure was used to avoid any damage to the PCM microcapsules due to shear and frictional forces that may develop during mechanical mixing. As such, this procedure enables discrimination of the effects of mechanical mixing from those associated with the nature of the chemical

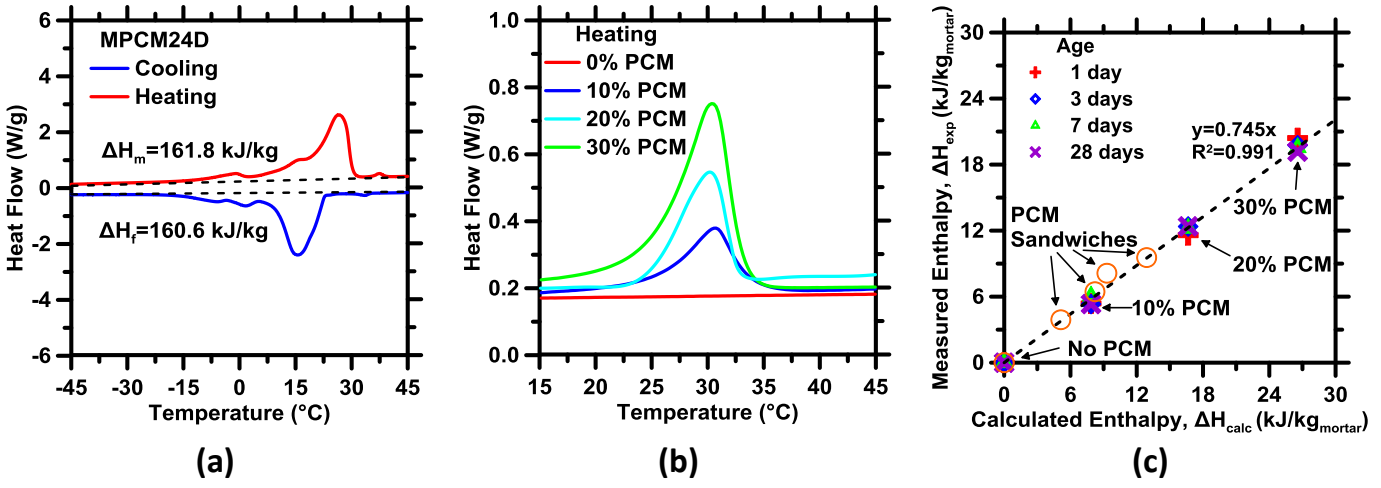

Fig. 2. **(a)** Representative DSC curves illustrating the enthalpy of melting and solidification of pristine MPCM24D. **(b)** Representative DSC curves for a PCM-mortar composites (w/c = 0.45) containing different volume fractions of MPCM24D. For clarity, only the endothermic (melting) peaks are shown, as the enthalpy of phase change measured during solidification is similar to that observed during melting. **(c)** The measured enthalpy of phase change for PCM-mortar composites (w/c = 0.45) as a function of the enthalpy that is expected based on the mass dosage of PCM in the composite (Equation (1)). Even when mechanical mixing is avoided (e.g., see data for PCM "sandwiches"), an enthalpy reduction is noted, indicating that mixing and mechanical damage caused to the PCM capsules is not the cause of enthalpy reduction.

environment. Fig. 2(c) reveals the measured enthalpy of phase change of these PCM sandwich composites falls on the same trend line as those subjected to mechanical mixing, indicating that mechanical mixing is not the cause of the observed enthalpy reduction. As such, this clarifies that a chemical rather than mechanical cause is at the origin of the enthalpy reduction observed in PCM containing cementitious composites.

Chemical stability of PCM within model cementitious environments: To evaluate the chemical stability of microencapsulated PCMs in alkaline conditions similar to cement pore solutions, PCM microcapsules were immersed in solutions of the following compositions: 0.02 M $Ca(OH)_2$, 0.5 M NaOH, 1 M NaOH, 2 M NaOH, and 3 M NaOH. Following 1, 3, 7, and 28 days of immersion, the enthalpy of phase change and the onset temperature of phase change of the PCM microcapsules were characterized via DSC.\

Fig. 3 shows the change in the enthalpy of phase change of MPCM24D and DS 5008X PCM microcapsules as a function of immersion time, relative to that in their pristine condition. Over 28 days of immersion, the enthalpy of phase change of the microencapsulated PCMs decreased by $\leq$ 2%. This suggests that the PCM capsule is sufficiently stable in alkaline environments. These results were consistent across PCMs of various transition temperatures (see Supplementary Materials, Section S.1). While these results indicate that negligible enthalpy reduction occurred in alkaline solutions, regardless of the associated cation, these simplified solutions did not contain the diversity of potentially deleterious ions present in the cement pore solution. For example, gypsum (hydrated calcium sulfate, $CaSO_4{\cdot}H_2O$) is commonly added to OPC to control the setting time. In this case, sulfate ions in the pore solution of cement paste may play an important role in deteriorating the PCM microcapsules' shell material, which requires further examination [42]. It should be noted that cement pore solution achieves gypsum saturation within the first few hours, and the concentration of sulfate ions progressively decreases in time [42].

Fig. 4(a) shows the relative change in enthalpy of phase change for MPCM24D microcapsules exposed to $CaSO_4{\cdot}2H_20$ (gypsum) solutions having concentrations of 7.35 mM, and 17.65 mM, for up to 28 days at 23 °C and 50 °C. The higher concentration, 17.65 mM corresponds to the solubility limit of gypsum in water at 23 °C. Also, while the lower temperature corresponds to ambient conditions, the higher temperature (50 °C) corresponds to that which may be achieved in modestly sized concrete sections due to the effects of self-insulation and the exothermic nature of cement + water reactions.

An immediate decrease in the PCM's enthalpy of phase change was observed (i.e., in $\leq$24 h) upon immersion in sulfate solutions, especially at slightly elevated temperature. For example, the enthalpy reduction of MPCM24D immersed in saturated calcium sulfate solution at 50 °C after 28 days was around 23%. These findings suggested that SO_4^{2-} ions play a significant role in inducing the observed 25% enthalpy reduction following embedment of PCM in cementitious composites (e.g., see Fig. 2(c)). This is attributed to the fact that the shell material of the microencapsulated PCMs was a melamine-formaldehyde (MF) resin that is synthesized by crosslinking melamine with formaldehyde under alkaline conditions. Since the crosslinking reactions are reversible, the crosslinks in MF's structure may breakdown in aqueous environments [43]. Following reversible breakdown, melamine co-crystallizes with SO_4^{2-} ions to form a melamine-sulfate (MS)-like supramolecular structure of molecular formula: $[(C_3H_7N_6^+)_2(SO_4^{2-})]{\cdot}2H_2O$ [44]. It is worth pointing out that the observed PCM enthalpy reduction occurred immediately after exposure to SO_4^{2-} ions – but after this initial reduction, no further change in the enthalpy of phase change was observed.

Fig. 4(b) shows XRD of MPCM24D samples before and following their immersion in saturated gypsum solutions for 28 days, and those for the melamine-sulfate (MS) supramolecular structure [44]. The X-ray patterns confirm the presence of supramolecular crystal compounds following immersion of PCM microcapsules in a saturated sulfate solution. It is postulated that hydrolysis of the MF crosslinks occurs within the shell of PCM microcapsules exposed to sulfate solutions. This process releases melamine, which then reacts with sulfate ions in solution to form the MS supramolecule with a 3D microporous structure that is linked by intermolecular hydrogen-bonds and aromatic π-π interactions [44]. These reactions deform and degrade the PCM's shell causing its rupture; after which the paraffinic core contacts the alkaline cementitious pore-fluid. This is confirmed by the SEM images presented in Fig. 4(c–d) which show capsule rupture following exposure to gypsum solutions. The reduction in the enthalpy of phase change is thus attributed to the contact of the PCM core material with the high pH cementitious environment. To confirm this hypothesis, the

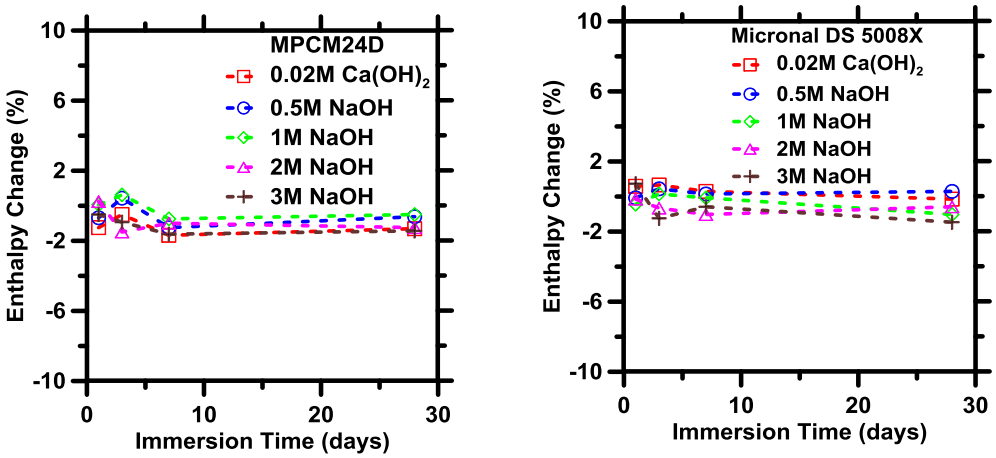

Fig. 3. The relative change in the enthalpy of phase change for **(a)** MPCM24D, and **(b)** Micronal DS 5008X following immersion in alkaline (similar to pore fluid) solutions for 28 days. The highest uncertainty in each measured data point is on the order of ±1%.

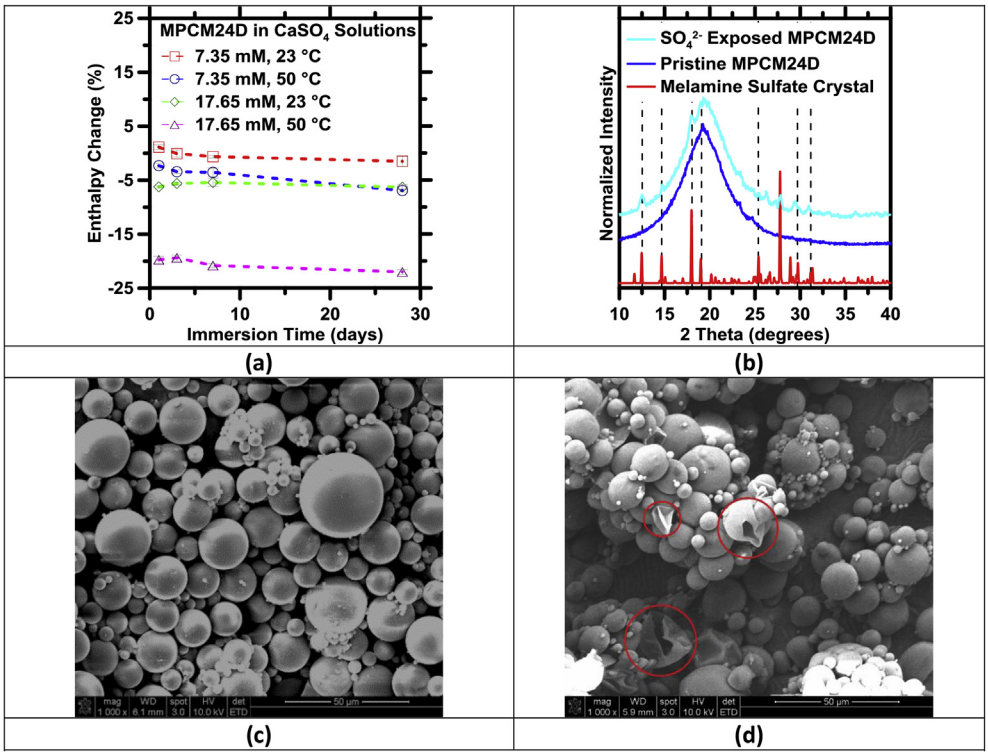

Fig. 4. **(a)** The change in the phase change enthalpy of MPCM24D following immersion in gypsum solutions. **(b)** The XRD patterns of the MS supramolecular structure and of MPCM24D before and after immersion in saturated gypsum solutions for 28 days. SEM images of the MPCM24D microcapsules: **(c)** before exposure, and, **(d)** after 3 days exposure to saturated calcium sulfate solution at 50 °C, wherein ruptured capsules are highlighted by the red circular traces. (For interpretation of the references to colour in this figure legend, the reader is referred to the web version of this article.)

paraffinic core material of MPCM24D was directly dispersed into gypsum solutions and stirred at 50 °C over a 28-day exposure period. Before exposure, the enthalpy of phase change of MPCM24D's core material was 199.8 kJ/kg; which indicated that following its encapsulation, the core accounted for 81 mass % of the MPCM24D microcapsules. Upon exposure to saturated gypsum solutions, the enthalpy of phase change of the core material decreased to 166.1 kJ/kg, a 17% reduction. Since the MF shell has no latent heat capacity, and the enthalpy reduction of MPCM24D immersed in at 50 °C after 28 days was ≈23% (e.g., see Fig. 4(a)), it was estimated that around 30% of the core material has been released (degraded) from the capsules. These results indicate that chemical reactions between the PCM core and SO_4^{2-} are primarily responsible for the observed enthalpy reduction (Fig. 2(c)). This pathway of the PCM's enthalpy reduction resulting from chemical interactions is summarized in Fig. 5.

3.2. Moisture transport behavior of PCM-containing cementitious composites

The water absorption response of PCM-mortars was quantified as per ASTM C1585. This involved measuring incremental mass

change (increase) of the samples after 1 min, 5 min, 10 min, 20 min, 30 min, 60 min, 120 min, 180 min, 240 min, 300 min, 360 min, and then every day for up to 8 days following their contact with water. The origin of time was taken at the moment when the specimen was first placed in contact with water. The cumulative volume of absorbed water per unit area of inflow surface I (in mm), was calculated as,

$$I = \frac{\Delta m_t}{\rho_w A} \tag{2}$$

where Δm_t (g) is the cumulative change in specimen mass at time t (seconds), A (mm^2) is the area of the specimen exposed to water, and ρ_w is the density of water (0.001 g/mm^3 at 23 °C). As per Hall [45], single-phase flow by capillary sorption in an unsaturated porous media can be expressed in the form of a diffusion equation – thus, from theory, I scales to $t^{1/2}$. But, in practice a finite positive intercept, k (mm), is noted as a result of the filling of surface porosity on the inflow surface [45]. As such, the sorptivity S can be determined from the slope of the best-fit line [38],

$$I = k + St^{1/2} \tag{3}$$

where S is the sorptivity of the material, i.e., the rate of absorption (in $mm/h^{1/2}$) and t is the time (in h). As per ASTM C1585, Equation (3) was fitted to the measured absorption data $I(t)$ within the first 6 h, and between 1 and 8 days, to calculate the initial sorptivity (S_1, in $mm/h^{1/2}$) and secondary sorptivity (S_2, in $mm/h^{1/2}$), respectively.

Fig. 6(a) shows representative water absorption data for a plain cement paste (w/c = 0.45) [38,46]. Neithalath [47] proposed that water sorption data can be described by a combination of an exponential term for sorption and a solution of Fick's second law for diffusion to predict time-dependent moisture ingress such that,

$$\begin{aligned} I &= \frac{\Delta m_t}{\rho_w A} \\ &= B\left[1 - \exp\left(\frac{-S_1 t^{1/2}}{B}\right)\right] + \frac{C_0 L}{\rho_w}\left\{1 \right. \\ &\quad \left. - \sum_{n=0}^{\infty} \frac{8}{(2n+1)^2 \pi^2} \exp\left[\frac{-D_m (2n+1)^2 \pi^2 t}{4L^2}\right]\right\} \end{aligned} \tag{4}$$

where B describes the penetration depth when capillary pores dominate initial sorption (mm), C_0 is the concentration of moisture at the specimen's surface (kg/m^3), D_m is the moisture diffusion coefficient (m^2/h), and L is the length of the specimen (m). Experimental data of I estimated using Equation (2), and S_1 obtained via Equation (3) were used to fit Equation (4), thus revealing the constants B, C_0, and D_m. Fig. 6(b) displays a representative fit of the Equation (4) for the plain paste (w/c = 0.45) including the separated contributions of capillary sorption and of diffusion, respectively. As expected, the contribution of capillary sorption to moisture intake was dominant at early times, and vanished over time, while the diffusion term represented long-term moisture transport involving the smaller gel pores [46,47]. The fitting of Equation (4) to the experimental water intake of the cement mortars (for w/c = 0.45) containing various dosages of PCM's and/or quartz inclusions was carried out (see Supplementary Materials, Section S.2). Note that, based on Equation (4), after an infinite amount of time, the cumulative water absorbed in the specimen is equal to $B + C_0 L/\rho_w$.

Fig. 7(a) displays the initial S_1 and secondary S_2 sorptivities measured for all mixtures (for w/c = 0.45) as functions of inclusion volume fraction ϕ_{P+Q}. It is noted that regardless of the nature of inclusions present (i.e., PCM or quartz), both S_1 and S_2 decreased linearly with increasing total inclusion volume fraction. This is because both quartz and PCM serve as non-sorptive inclusions [48]. As the volume fraction of non-sorptive inclusions increases, capillary flow is redirected around inclusion particles, increasing the tortuosity of the transport path. As a result, moisture penetration rates diminish. Further, the initial sorptivity decreased faster than the secondary sorptivity, indicating a greater relative importance of diffusive moisture transport with increasing inclusion dosage. In addition, the effective moisture diffusion coefficient D_m (Fig. 7(b)) decreased systematically with inclusion dosage since both PCM and quartz were non-porous inclusions, far less permeable than the cement paste. In turn, the total amount of water absorbed by the composites diminished with inclusion dosage due to the dilution of the content of porous cement paste, which is the main water-sorbing component in the composite (see Fig. 7(c)).

As water absorption appeared relatively insensitive to the type of inclusion, a model was sought to capture both the effects of w/c and inclusion volume (i.e., reduction in paste content) on water absorption. Simply, water absorption depends on the unsaturated and interconnected porosity of the system, i.e., the volume available to be filled with water. The total porosity, composed of capillary porosity (V_{cw}), the gel porosity (V_{gw}), and chemical shrinkage (V_{cs}) in a cement paste can be determined by Powers' model which estimates the volume relationships among constituents and porosity of the mixtures during the hydration process [49,50] at a

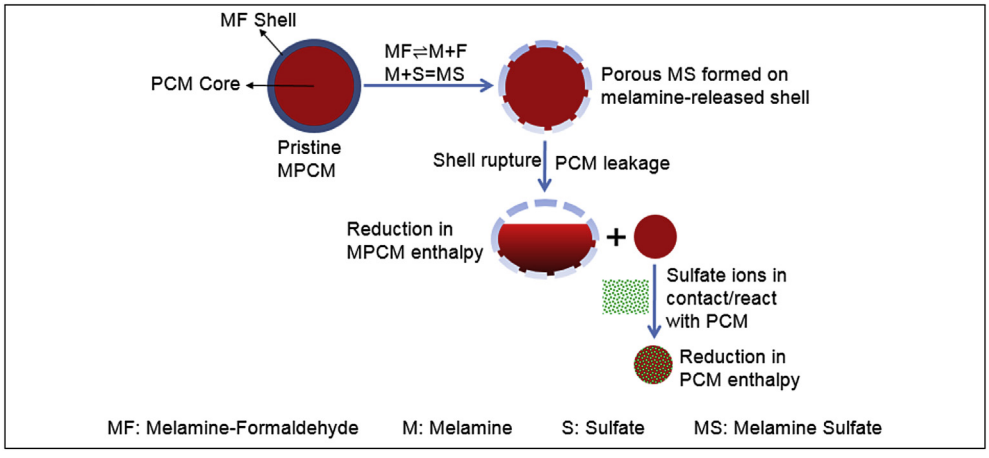

Fig. 5. The proposed chemical interaction pathway which results in enthalpy reduction (reduction) of the PCMs following exposure to caustic solutions containing SO_4^{2-} ions.

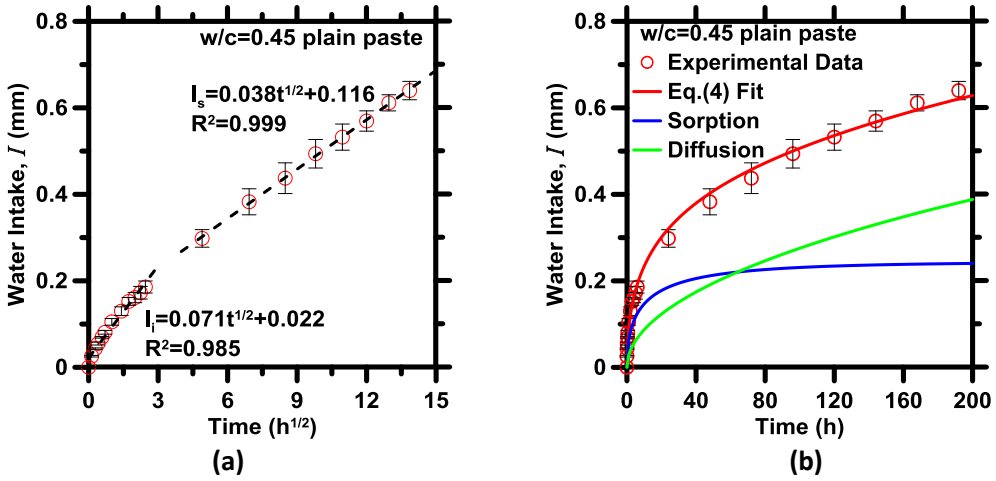

Fig. 6. **(a)** Water sorption as a function of the square root of time ($h^{1/2}$) for a plain cement (w/c = 0.45), and **(b)** Representative fits of the sorption-diffusion equation (Equation (4)) to the plain cement paste's water sorption response.

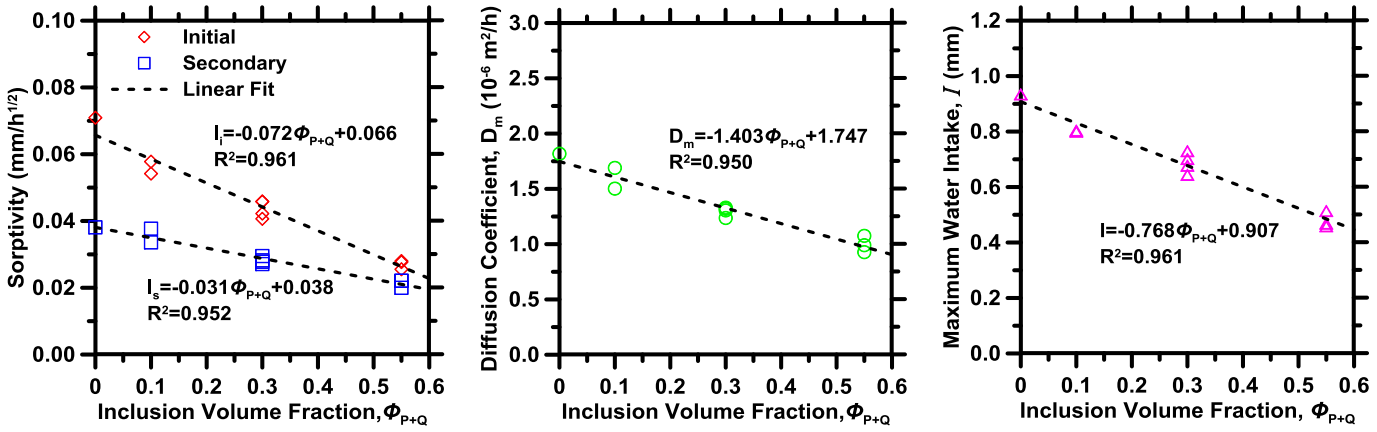

Fig. 7. **(a)** Water sorptivity, **(b)** Moisture diffusion coefficients of cementitious composites containing PCM and/or quartz inclusions for w/c = 0.45, and **(c)** The cumulative amount of water absorbed by cementitious composites containing PCM and/or quartz inclusions for w/c = 0.45 after infinite time.

given degree of cement reaction, here taken to be 80% after 28 days [51].

Since both PCM and quartz were non-sorptive and non-reactive inclusions, and assuming that no volume expansion occurs during wetting, the total porosity of the mixture can be calculated as a function of w/c, degree of reaction (α, unitless), and the inclusion dosage. Indeed, isothermal calorimetry has indicated that PCM microcapsules and quartz inclusions exert no appreciable effect on the degree of hydration [12]. As such, Fig. 8 shows the maximum long-term water uptake of a range of cementitious composites (i.e., both with, and without inclusions) as a function of their total porosity calculated by Powers model [49]. Across all compositions, an empirical logarithmic expression described the relationship between the maximum water uptake I_{max} and the total porosity V_{tot} (i.e., the sum of the capillary and gel pores, and void spaces created by chemical shrinkage):

$$I_{max} = 0.50 \ln V_{tot} + 1.36 \quad (5)$$

To ascertain the predictive power of this approach, water sorption experiments were carried out on three additional mixtures having different w/c and volume fractions of PCM and quartz: (i) w/c = 0.40 mortar containing 40 vol % PCM, (ii) w/c = 0.50 mortar containing 25 vol % PCM and 25 vol % quartz, and (iii) w/c = 0.60 mortar containing 25 vol % quartz. The empirical expression shown in Equation (5) was able to robustly capture the terminal amount of water sorbed by these mixtures, simply from knowledge of the mixture proportions, and the degree of reaction (see Fig. 8). It should be noted that Equation (5) accounts for differences in porosity (volume fraction) based only on the initial w/c of the cement paste. The addition of non-sorptive inclusions dilutes the volume fraction of the porous cement paste, thereby reducing the volume of porosity in the cementitious composite. Therefore, the present expression only accounts for the effects of non-sorptive (or negligibly sorptive) inclusions. While Equation (5) could indeed be modified to represent the effects of porous aggregates, i.e., by taking aggregate porosity into account in the porosity volume fraction parameter V_{tot} – this approach was not implemented here. As such, it is possible to estimate terminal water sorption from the porosity of the material. Of course, the results indicate that PCMs diminish water sorption similar to other non-porous inclusions, an effect that is caused on account of dilution of the cement paste content.

3.3. Unrestrained drying shrinkage of cementitious composites containing PCMs

Fig. 9 shows the drying shrinkage strain (*S*, με) of cementitious

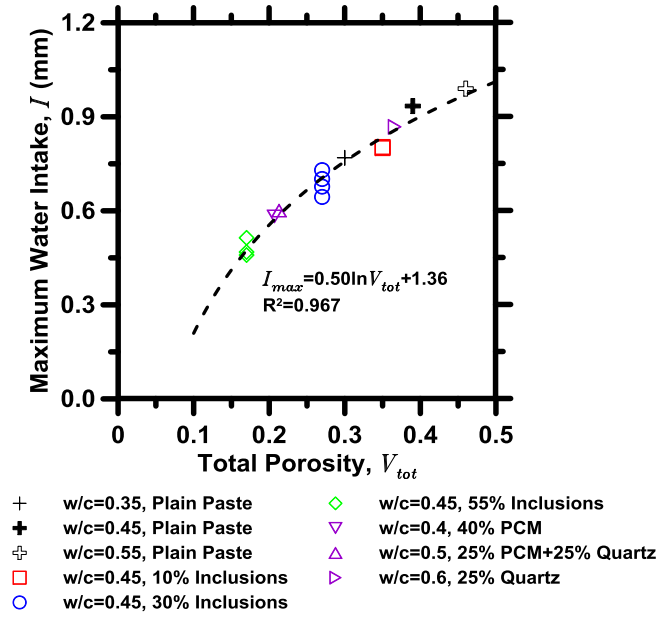

Fig. 8. The maximum water intake at infinite time (I_{max}) as a function of total porosity, V_{tot} calculated using Powers model [48].

composites containing PCM and/or quartz inclusions as a function of time, for w/c = 0.45. For both quartz mortars and mixed mortars (i.e., those containing both quartz and PCM inclusions), increasing the quartz volume fraction reduced drying shrinkage, since stiff inclusions restrain the shrinkage of the paste [12]. The dosage of microencapsulated PCM inclusions resulted in no change in shrinkage, vis-à-vis the plain cement paste. This is because the soft PCM inclusions, due to their compliant nature, are unable to restrain the shrinkage of the cement paste upon drying. This is supported by the observation that, when PCM and quartz inclusions were dosed together, the measured shrinkage response was similar to that expected for a mixture containing only quartz inclusions.

To better understand the trends in shrinkage, and the influence of the inclusion properties, the model of Hobbs developed for two-component composites (i.e., matrix + inclusion) was applied to predict the shrinkage of the composite [29,52]. This model is expressed as [29],

$$S_{m+i} = S_m - \frac{2K_i(S_m - S_i)\phi_i}{K_i + K_m + (K_i - K_m)\phi_i} \quad \text{with} \quad K_j = \frac{E_j}{3(1-2\upsilon_j)} \tag{6}$$

where S_j, K_j, E_j, and υ_j are the shrinkage strain, bulk modulus, modulus of elasticity, and Poisson's ratio of component *j of volume fraction* ϕ_j, respectively. Here, the subscripts $m + i$, m, and i refer to the two-component composite, the matrix (cement paste), and the inclusions (PCM or quartz), respectively. The shrinkage of PCM microcapsules was assumed to be near-equivalent to that of the cement paste, and quartz was assumed to be non-shrinking [12], Therefore the shrinkage ratio of quartz and PCM inclusions in relation to cement paste are taken as: $S_Q/S_m = 0.01$ and $S_P/S_m = 0.99$. The bulk modulus of the cement paste was calculated: (i) from measured data of its modulus of elasticity $E_m = 9.58$ GPa, 13.48 GPa, 15.65 GPa, and 16.75 GPa [52] at ages of 1, 3, 7, and 28 days, respectively and (ii) assuming its Poisson's ratio to be $\upsilon_m = 0.2$ [53]. The modulus of elasticity and Poisson's ratio of the microencapsulated PCM and quartz inclusions were estimated based on literature data as: $E_P = 0.0557$ GPa, $\upsilon_P = 0.499$ [54], and $E_Q = 72$ GPa, $\upsilon_Q = 0.22$ [55], respectively. The Hobbs model assumes the following: (i) the cementitious composites consist of only two phases (i.e., inclusion particles dispersed in a continuous cement paste matrix), (ii) the inclusions and cement paste matrix are elastic, and (iii) the elastic properties of the components do not change with shrinkage.

For three-component systems (PCM microcapsules + quartz + cement paste), a two-step approach was applied to calculate the shrinkage strain via the Hobbs model. In this approach, the PCM and cement paste were treated as a *homogeneous* matrix into which quartz inclusions were embedded. The effective modulus of elasticity of the cement paste embedded with PCMs was computed using Hobbs model (for modulus of elasticity) as [29],

$$E_{m+P} = \frac{(1-2\upsilon_{m+P})\left(1-\frac{\varphi_P}{1-\varphi_Q}\right)E_m}{(1-2\upsilon_m)\left(1+\frac{\varphi_P}{1-\varphi_Q}\right)} \tag{7}$$

where E_{m+P} is the effective modulus of elasticity of the paste + PCM composite, and E_m and E_P are the moduli of elasticity of the cement paste matrix and microencapsulated PCM, respectively. The corresponding effective Poisson's ratio of the composite, υ_{m+P} was calculated based on the Reuss-Voigt-Hill average [56] as,

$$\upsilon_{m+P} = \left[\left(\upsilon_P\frac{\phi_P}{1-\phi_Q} + \upsilon_m\frac{\phi_m}{1-\phi_Q}\right) + \left(\frac{\upsilon_P\upsilon_m}{\upsilon_P\frac{\phi_m}{1-\phi_Q} + \upsilon_m\frac{\phi_P}{1-\phi_Q}}\right)\right] \Big/ 2 \tag{8}$$

It should be noted that Hobbs model noted in Equation (7) was derived for a case of considerable mismatch between the Poisson's ratios of the components, and assumed that inclusions had a negligible modulus of elasticity compared to that of the matrix (such that $E_i \approx 0$, and $S_i/S_m \approx 1$). As such, instead of homogenizing quartz and cement paste as the matrix, quartz was treated as inclusion and embedded into a matrix composed of PCM microcapsules and cement paste. The effective modulus of elasticity E_{m+P} and Poisson's ratio υ_{m+P} of the homogenized PCM + cement paste composite were used to calculate its effective bulk modulus (K_{m+P}). This served as an input in Equation (6) for K_m while the quartz particles were treated as rigid inclusions. Based on these guidelines, the drying shrinkage of a three-component composite, S_{m+P+Q}, was predicted as,

$$\frac{S_{m+P+Q}}{S_{m+P}} = 1 - \frac{\frac{2E_Q\phi_Q}{1-2\upsilon_Q}\left(1-\frac{S_Q}{S_{m+P}}\right)}{\frac{E_Q}{1-2\upsilon_Q} + \frac{E_{m+P}}{1-2\upsilon_{m+P}} + \left(\frac{E_Q}{1-2\upsilon_Q} - \frac{E_{m+P}}{1-2\upsilon_{m+P}}\right)\phi_Q} \tag{9}$$

where S_{m+P} was obtained as a function of S_m by Equation (6). Fig. 10 shows the measured and predicted shrinkage strains of PCM and/or quartz containing composites normalized by that of plain paste shrinkage, S_m, after 28 days of drying. It is noted that Hobbs model can accurately predict the shrinkage of composites containing both stiff, and/or compliant inclusions. The results indicate that, broadly, PCMs do not restrain paste shrinkage, and fulfill a role similar to air-voids (i.e., in the context of shrinkage) in the system. This is significant as while PCM microcapsules do not reduce shrinkage, in spite of the effects of dilution (i.e., a reduction in paste content), when dosed with quartz inclusions, only the latter serve as a shrinkage restraining agent. Nevertheless, since PCMs are expected to be dosed as replacement of fine mineral aggregates, the overall

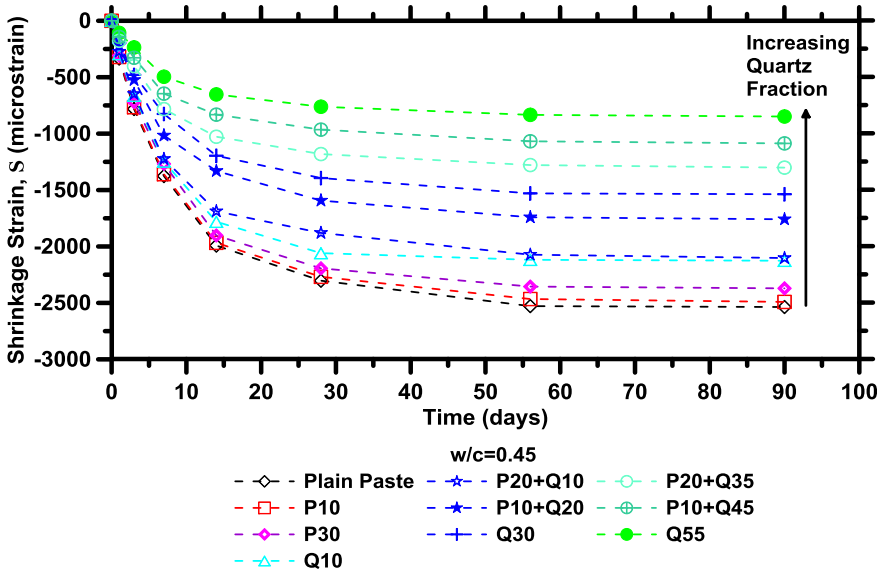

Fig. 9. Shrinkage plotted against the drying time for samples containing different volume fractions of PCM and/or quartz.

shrinkage that develops can be adjusted by the dosage of stiff inclusions present in the mixture.

It is worth pointing out that in practical applications the effect of temperature cycling on the expansion and shrinkage of the PCM capsules may be relevant. While it is well known that thermal expansion and shrinkage of the PCM's paraffin core is much higher than that of the MF shell, typically, the PCM capsules are only partially filled with core material to account for the thermal expansion mismatch of the core and shell components. In fact, other research has revealed that the effective coefficient of thermal expansion of the PCM microcapsules (core + shell) is similar to that of the encapsulation (shell) material [57]. Since the coefficient of thermal expansion of the shell is on the same order as that of the cement paste matrix, this ensures that no damage would occur at the interface between the cement paste and the microcapsules when temperature changes – more so since the shell is around an order of magnitude less stiff than the cement paste matrix. As such, the addition of microencapsulated PCMs is expected to exert no detrimental effect on volume changes of cementitious composites.

4. Summary and conclusions

This study has investigated how the dosage of microencapsulated PCMs influences the durability of cementitious materials. It is noted that, while PCMs remain unaffected in alkaline solutions, they experience a significant enthalpy reduction, on the order of 25%, when exposed to sulfate-bearing environments. The mechanism of such enthalpy reduction was identified as hydrolysis of the melamine-formaldehyde PCM capsule followed by its reaction with sulfate ions to form a melamine-sulfate supramolecular crystal. These reactions result in shell rupture following which the paraffinic PCM core too contacts sulfate ions, resulting in enthalpy reduction. With regards to water sorption, PCMs serve as a non-sorptive inclusion similar to graded quartz sand. Therefore, increasing the volume fraction of either inclusion reduced the volume of water sorbed, and the rate of water sorption. These effects, especially the extent of terminal water sorption, can be estimated for the case of non-sorptive inclusions using Powers' model [49]. Furthermore, the drying shrinkage of cementitious composites was essentially unaltered by the presence of PCMs, as such compliant inclusions are unable to offer any resistance to the

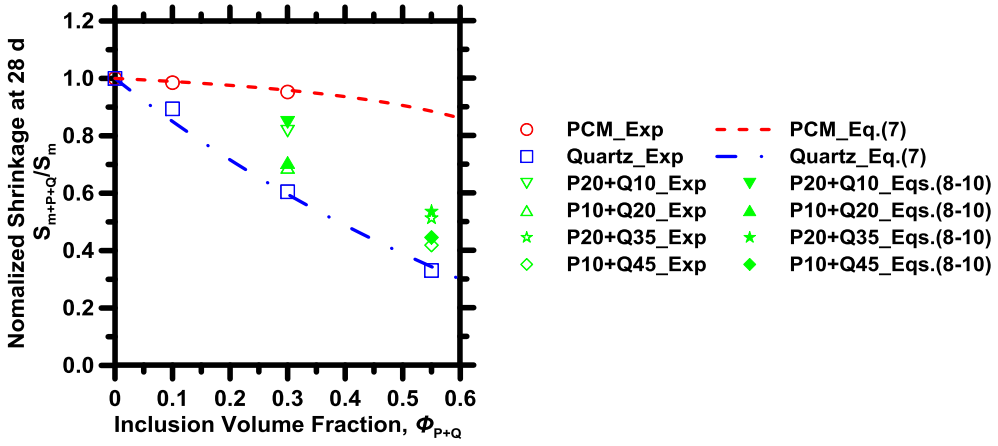

Fig. 10. A comparison of measured and modeled drying shrinkage data of all cementitious mixtures after 28 days of drying, normalized by shrinkage of plain paste with w/c = 0.45.

cement paste's shrinkage. On the other hand, stiff quartz inclusions reduced shrinkage significantly – due to the effects of aggregate restraint. The model of Hobbs is able to properly capture the effects of both, inclusion stiffness and volume fraction, providing a means to estimate the shrinkage of cementitious composites containing such inclusions. In general, it is noted that, while PCMs may themselves be detrimentally impacted in sulfate-containing cementitious environments, they do not in any way detrimentally impact the durability of cementitious composites in which they are embedded.

Acknowledgements

The authors acknowledge financial support for this research provisioned via an Infravation ERA-NET Plus Grant (31109806.0001), the National Science Foundation (CMMI: 1130028, CAREER: 1253269) and California Energy Commission (Contract: PIR: 12-032). The authors also kindly acknowledge financial support provided by The Sustainable L.A. Grand Challenge and Office of the Vice-Chancellor for Research at UCLA. The contents of this paper reflect the views and opinions of the authors, who are responsible for the accuracy of datasets presented herein. The Laboratory for the Chemistry of Construction Materials (LC^2) and the Molecular Instrumentation Center at UCLA gratefully acknowledge the support that has made their operations possible.

Appendix A. Supplementary data

Supplementary data related to this article can be found at http://dx.doi.org/10.1016/j.cemconcomp.2017.04.010.

References

[1] M. Isaac, D.P. van Vuuren, Modeling global residential sector energy demand for heating and air conditioning in the context of climate change, Energy Policy 37 (2009) 507–521.
[2] M.M. Farid, A.M. Khudhair, S.A.K. Razack, S. Al-Hallaj, A review on phase change energy storage: materials and applications, Energy Convers. Manage 45 (2004) 1597–1615.
[3] A.M. Khudhair, M.M. Farid, A review on energy conservation in building applications with thermal storage by latent heat using phase change materials, Energy Convers. Manage 45 (2004) 263–275.
[4] E. Oro, A. de Gracia, A. Castell, M.M. Farid, L.F. Cabeza, Review on phase change materials (PCMs) for cold thermal energy storage applications, Appl. Energy 99 (2012) 513–533.
[5] B. Zalba, J.M. Marin, L.F. Cabeza, H. Mehling, Review on thermal energy storage with phase change: materials, heat transfer analysis and applications, Appl. Therm. Eng. 23 (2003) 251–283.
[6] A.M. Thiele, Z. Wei, G. Falzone, B.A. Young, N. Neithalath, G. Sant, L. Pilon, Figure of merit for the thermal performance of cementitious composites containing phase change materials, Cem. Concr. Comp. 65 (2016) 214–226.
[7] D.W. Zhang, H. Furuuchi, A. Hori, T. Ueda, Fatigue degradation properties of PCM-concrete interface, J. Adv. Concr. Technol. 7 (2009) 425–438.
[8] J.-F. Su, X.-Y. Wang, H. Dong, Micromechanical properties of melamine-formaldehyde microcapsules by nanoindentation: effect of size and shell thickness, Mater. Lett. 89 (2012) 1–4.
[9] W. Li, G. Song, G. Tang, X. Chu, S. Ma, C. Liu, Morphology, structure and thermal stability of microencapsulated phase change material with copolymer shell, Energy 36 (2011) 785–791.
[10] M. Aguayo, S. Das, A. Maroli, N. Kabay, J.C.E. Mertens, S.D. Rajan, G. Sant, N. Chawla, N. Neithalath, The influence of microencapsulated phase change material (PCM) characteristics on the microstructure and strength of cementitious composites: experiments and finite element simulations, Cem. Concr. Comp. 73 (2016) 29–41.
[11] J. Chen, F.J. Liu, Y.F. Zheng, Review on phase change material slurries, Adv. Mater. Res. 860–863 (2014) 946–951.
[12] F. Fernandes, S. Manari, M. Aguayo, K. Santos, T. Oey, Z. Wei, G. Falzone, N. Neithalath, G. Sant, On the feasibility of using phase change materials (PCMs) to mitigate thermal cracking in cementitious materials, Cem. Concr. Comp. 51 (2014) 14–26.
[13] P. Meshgin, Y. Xi, Y. Li, Utilization of phase change materials and rubber particles to improve thermal and mechanical properties of mortar, Constr. Build. Mater 28 (2012) 713–721.
[14] M. Hunger, A.G. Entrop, I. Mandilaras, H.J.H. Brouwers, M. Founti, The behavior of self-compacting concrete containing micro-encapsulated phase change materials, Cem. Concr. Res. 31 (2009) 731–743.
[15] A. Sari, Thermal reliability test of some fatty acids as PCMs used for solar thermal latent heat storage applications, Energy Convers. Manage 44 (2003) 2277–2287.
[16] J. Skalny, I. Jawed, H.F.W. Taylor, Studies on hydration of cement: recent developments, World Cem. Technol. 8 (1978) 183–186.
[17] G.C. Bye, Portland Cement: Composition, Production and Properties, Thomas Telford Publishing, London, 1999.
[18] J.W. Bullard, H.M. Jennings, R.A. Livingston, A. Nonat, G.W. Scherer, J.S. Schweitzer, K.L. Scrivener, J.J. Thomas, Mechanisms of cement hydration, Cem. Concr. Res. 41 (2011) 1208–1223.
[19] D.E. Macphee, E.E. Lachowski, A.H. Taylor, T.J. Brown, Microstructural development in pore reduced cement (PRC), in: MRS Proceedings, vol. 245, 1991, pp. 303–308.
[20] S.C. Taylor, W.D. Hoff, M.A. Wilson, K.M. Green, Anomalous water transport properties of Portland and blended cement-based materials, J. Mater. Sci. Lett. 18 (1999) 1925–1927.
[21] D.R.M. Brew, F.C. de Beer, M.J. Radebe, R. Nshimirimana, P.J. McGlinn, L.P. Aldridge, T.E. Payne, Water transport through cement-based barriers-A preliminary study using neutron radiography and tomography, Nucl. Instrum. Methods Phys. Res. A 605 (2009) 163–166.
[22] R. Henkensiefken, J. Castro, D. Bentz, T. Nantung, J. Weiss, Water absorption in internally cured mortar made with water-filled lightweight aggregate, Cem. Concr. Res. 39 (2009) 883–892.
[23] J. Castro, D. Bentz, J. Weiss, Effect of sample conditioning on the water absorption of concrete, Cem. Concr. Comp. 33 (2011) 805–813.
[24] C. Hall, W.D. Hoff, S.C. Taylor, M.A. Wilson, B.G. Yoon, H.W. Reinhardt, M. Sosoro, P. Meredith, A.M. Donald, Water anomaly in capillary liquid absorption by cement-based materials, J. Mater. Sci. Lett. 14 (1995) 1178–1181.
[25] L.C. Wang, Analytical methods for prediction of water absorption in cement-based material, China Ocean. Eng. 23 (2009) 719–728.
[26] A.L. Stockett, A.M. Schneide, F.J. Mardulie, An analysis of drying shrinkage data for Portland cement mortar and concrete, J. Mater 2 (1967) 829–842.
[27] J. Bisschop, J.G.M. van Mier, Effect of aggregates on drying shrinkage micro-cracking in cement-based composites, Mater. Struct. 35 (2002) 453–461.
[28] S.D. Abyaneh, H.S. Wong, N.R. Buenfeld, Computational investigation of capillary absorption in concrete using a three-dimensional mesoscale approach, Comput. Mater. Sci. 87 (2014) 54–64.
[29] D.W. Hobbs, The dependence of the bulk modulus, Young's modulus, creep, shrinkage, and thermal expansion of concrete upon aggregate volume concentration, Mater. Struct. 4 (1971) 107–114.
[30] A.R. Sakulich, D.P. Bentz, Increasing the service life of bridge decks by incorporating phase-change materials to reduce freeze-thaw cycles, J. Mater. Civ. Eng. 24 (2012) 1034–1042.
[31] ASTM Standard C150/C150M: Standard Specification for Portland Cement, ASTM International, West Conshohocken, PA, 2016.
[32] ASTM Standard C192/C192M: Standard Practice for Making and Curing Concrete Test Specimens in the Laboratory, ASTM International, West Conshohocken, PA, 2012.
[33] ASTM Standard C778: Standard Specification for Standard Sand, ASTM International, West Conshohocken, PA, 2013.
[34] C.F. Ferraris, V.A. Hackley, A.I. Avilés, Measurement of particle size distribution in portland cement powder: analysis of ASTM round robin studies, Cem. Concr. Aggreg 26 (2004) 1–11.
[35] G. Gao, S. Moya, H. Lichtenfeld, A. Casoli, H. Fiedler, E. Donath, H. Mohwald, The decomposition process of melamine formaldehyde cores: the key step in the fabrication of ultrathin polyelectrolyte multilayer capsules, Macromol. Mater. Eng. 286 (2001) 355–361.
[36] G. Ghosh, Dispersion-equation coefficients for the refractive index and birefringence of calcite and quartz crystals, Opt. Commun. 163 (1999) 95–102.
[37] ASTM Standard E1269: Standard Test Method for Determining Specific Heat Capacity by Differential Scanning Calorimetry, ASTM International, West Conshohocken, PA, 2011.
[38] ASTM Standard C1585: Standard Test Method for Measurement of Rate of Absorption of Water by Hydraulic-cement Concretes, ASTM International, West Conshohocken, PA, 2012.
[39] ASTM Standard C157: Standard Test Method for Length Change of Hardened Hydraulic-cement Mortar and Concrete, ASTM International, West Conshohocken, PA, 2014.
[40] N. Ukrainczyk, S. Kurajica, J. Sipusic, Thermophysical comparison of five commercial paraffin waxes as latent heat storage materials, Chem. Biochem. Eng. Q. 24 (2010) 129–137.
[41] ASTM Standard C305: Standard Practice for Mechanical Mixing of Hydraulic Cement Pastes and Mortars of Plastic Consistency, ASTM International, West Conshohocken, PA, 2014.
[42] S. Mindess, J.F. Young, D. Darwin, Concrete, second ed., Prentice Hall, New Jersey, 2003.
[43] D.R. Bauer, Melamine Formaldehyde cross-linker: characterization, network formation and cross-link degradation, Prog. Org. Coat. 14 (1986) 193–218.
[44] X.H. Li, S.Z. Yang, W.D. Xiang, Q. Shi, A novel porous supramolecular complex constructed by the co-crystallization of melamine and sulfate via hydrogen bonds and aromatic pi-pi interaction, Struct. Chem. 18 (2007) 661–666.
[45] C. Hall, Water sorptivity of mortars and concretes: a review, Mag. Concr. Res. 41 (1989) 51–61.
[46] Y. Xi, Z.P. Bažant, L. Molina, H.M. Jennings, Moisture diffusion in cementitious

materials Moisture capacity and diffusivity, Adv. Cem. Based Mater 1 (1994) 258–266.
[47] N. Neithalath, Analysis of moisture transport in mortars and concrete using sorption-diffusion approach, ACI Mater. J. 103 (2006) 209–217.
[48] C. Hall, W.D. Hoff, M.A. Wilson, Effect of nonsorptive inclusions on capillary absorption by a porous material, J. Phys. D. Appl. Phys. 26 (1993) 31–34.
[49] T.C. Powers, T.L. Brownyard, Studies of the physical properties of hardened portland cement paste, J. Am. Concr. Inst. Proc. 43 (1947) 469–504.
[50] O.M. Jensen, P.F. Hansen, Water-entrained cement-based materials I: principle and theoretical background, Cem. Concr. Res. 31 (2001) 647–654.
[51] J.F. Young, S. Mindess, A. Bentur, R. Gray, The Science and Technology of Civil Engineering Materials, Prentice Hall, New Jersey, 1998.
[52] G. Falzone, G. Puerta Falla, Z. Wei, M. Zhao, A. Kumar, M. Bauchy, N. Neithalath, L. Pilon, G. Sant, The influences of soft and stiff inclusions on the mechanical properties of cementitious composites, Cem. Concr. Comp. 71 (2016) 153–165.
[53] G. De Schutter, L. Taerwe, Degree of hydration-based description of mechanical properties of early age concrete, Mater. Struct. 29 (1996) 335–344.
[54] M. Hossain, C. Ketata, Experimental study of physical and mechanical properties of natural and synthetic waxes using uniaxial compressive strength test, in: Proceedings of Third International Conference on Modeling, Simulations and Applied Optimalization, 2009, pp. 1–5.
[55] X.Q. Chen, S.L. Zhang, G.J. Wagner, W.Q. Ding, R.S. Ruoff, Mechanical resonance of quartz microfibers and boundary condition effects, J. Appl. Phys. 95 (2004) 4823–4828.
[56] R. Hill, The elastic behaviour of a crystalline aggregate, Proc. Phys. Soc. Sect. A 65 (1952) 349–354.
[57] B.A. Young, Z. Wei, J. Rubalcava-Cruz, G. Falzone, A. Kumar, N. Neithalath, G. Sant, L. Pilon, A general method for retrieving thermal deformation properties of microencapsulated phase change materials or other particulate inclusions in cementitious composites, Mater. Des. 126 (2017) 259–267.